

Modeling the Development of Metastases from Primary and Locally Recurrent Tumors: Comparison with a Clinical Data Base for Prostatic Cancer¹

E. D. Yorke,² Z. Fuks, L. Norton, W. Whitmore, and C. C. Ling

Division of Radiation Oncology and Biophysics, George Washington University Medical Center, Washington, DC 20037 [E. D. Y.], and Departments of Radiation Oncology [Z. F.], Medicine [L. N.], Surgery [W. W.], and Medical Physics [C. C. L.], Memorial Sloan Kettering Cancer Center, New York, New York 10021

ABSTRACT

For many types of cancer, patients who relapse locally following localized treatment such as surgery or radiation therapy are found to have a higher incidence of distant metastases than those who are locally controlled. In this study we developed a mathematical model to investigate whether the excess distant metastases arise mainly from the local recurrence or whether the primary tumors in this group of patients have an intrinsically higher metastatic potential than those of locally controlled patients of the same clinical stage. The parameters of the model were chosen to be representative of prostate cancer and the calculated results were compared with published clinical data for carcinoma of the prostate. The best agreement with the data was seen for parameters which imply somewhat more "aggressive" primary tumors for locally relapsing patients, yielding relatively high rates of micrometastatic dissemination prior to initial diagnosis. However, the model calculations indicate that more than half of the metastases in such patients originated in association with the development of a local recurrence. Therefore, achieving local control in this group of patients would be beneficial in improving long term survival.

INTRODUCTION

Developments and improvements in localized cancer therapy such as the introduction of three-dimensional conformal radiation therapy (1-3) may lead to higher local control rates. However, the majority of cancer deaths result from metastatic disease and it is not known whether enhanced local control will result in an improvement in long term survival and cure.

It has been estimated that approximately one third of the patients who present with localized disease and are treated with curative radiation therapy fail initially at the primary tumor site (4), and many of these patients subsequently develop metastatic disease (5, 6). If micrometastases are present at the time of diagnosis in these patients then they will eventually exhibit distant metastases regardless of the outcome of their local treatment. However, if the majority of the distant metastases in this group of patients arise from the locally recurrent tumor, achieving local control will have a strong impact on long term survival (1, 2), in part by lowering the incidence of distant metastases.

Clinical data (7, 8) and animal experiments (9-11) clearly demonstrate that local failure is associated with increased incidence of distant metastases. Some of the animal experiments also indicate that the recurrent tumor is more effective than the primary tumor in producing metastases. For example, Ramsay *et al.* (9) investigated mice bearing transplanted squamous cell carcinomas on a leg. When the tumor reached 6 mm in diameter, the leg was either amputated or given a sufficiently large radiation dose to produce 50% tumor control. If the tumor recurred locally, it was permitted to regrow to 6 mm and then the leg was amputated. The incidence of distant metastases for the locally controlled animals was 6.9%, regardless of whether control

was achieved by surgery or radiation, while 43% of the locally failed animals developed distant metastases. Given that the same tumor and host model were used throughout, it is unlikely that experimental uncertainty could account for the 6-fold difference in metastatic disease between the two cohorts of animals. This and other animal experiments (10, 11), as well as immunohistochemical and molecular studies (7, 8), indicate that changes in cell phenotype as the tumor progresses may give the locally recurrent tumor a higher metastatic potential than the primary tumor.

There have been several retrospective clinical studies analyzing patterns of failure after definitive local treatment. Fuks *et al.* (12) reviewed 679 patients with node-negative stage B-C carcinoma of the prostate treated with permanent retropubic ¹²⁵I implants. The most significant factor affecting distant failure was local control. The criteria for local failure included both clinical indicators and positive biopsy at 1 year or longer after implantation, even in the absence of clinical evidence of local progression (12). Actuarial 15-year distant metastasis-free survival in 351 locally controlled patients was 77%, while in 328 patients with local relapse it was 24%. In this study, it was also demonstrated that distant metastases occurred earlier in the locally controlled patients than in the local failures (median of 37 months *versus* median of 54 months). Leibel *et al.* (13) found a significant increase in the incidence of distant metastases for patients with local relapse, relative to patients with local control, for tumors of the oral cavity, oropharynx, supraglottic larynx, and glottis but not for nasopharynx and hypopharynx tumors. Retrospective studies for T1-N0 breast tumors (14, 15), T1-2N0 non-small cell lung cancer (16-18), and a spectrum of other human tumors (19-31) have also reported higher rates of distant metastases in patients with local relapse.

It is more difficult to interpret the clinical studies than the animal models. The majority of excess distant metastases may arise from the locally recurrent tumor. However, it has also been suggested that both the excess distant metastases and the local recurrence arise because the primary tumor is of a particularly aggressive nature and is both resistant to local control and more prone to metastasize.

To assist in sorting out these alternatives for carcinoma of the prostate, we developed a mathematical model that describes the growth of the primary tumor and the development of metastases in patients with local control and in patients with local relapse. Within the framework of this model, we used two techniques. The first was a combination of analytical and numerical integration calculations, which we have termed the deterministic version of the model. The second, the simulation version, was a Monte Carlo-like simulation from which we generated curves of DMFS³ as a function of time. While the simulation version requires fewer assumptions, it is more flexible and can yield more detailed information. The deterministic version is more easily implemented with a small computer (indeed, if exponential growth kinetics are used, hand calculations are possible). Therefore, we shall present both versions of the model below. Parameters relating to tumor growth kinetics and detectable sizes were obtained from clinical data for prostatic cancer. Parameters describing the metastatic capability of the tumor were varied and the time de-

Received 1/12/93; accepted 4/23/93.

The costs of publication of this article were defrayed in part by the payment of page charges. This article must therefore be hereby marked *advertisement* in accordance with 18 U.S.C. Section 1734 solely to indicate this fact.

¹ Supported in part by Grant CA59017 from the National Cancer Institute, NIH, DHHS.

² To whom requests for reprints should be addressed.

³ The abbreviation used is: DMFS, distant metastasis-free survival.

pendence of DMFS was compared with the clinical data previously published by us (12). The model provides a possible interpretation of the clinical results relative to the role of local control in achieving long term distant metastasis-free survival.

MATERIALS AND METHODS

Tumor Kinetics. Two functions have been widely used in the literature to model tumor growth. In the exponential growth model (32) the number of tumor cells at time t , $n(t)$, is a function of the initial cell number N_0 and the growth constant λ ,

$$n(t) = N_0 \exp(\lambda t) \tag{1}$$

However, often the exponential function does not describe the rate of tumor growth *in vivo*, which slows as the tumor size increases. These observed kinetics are better fit by the three-parameter Gompertzian function (33–36)

$$n(t) = N_\infty \exp\left(\ln\left(\frac{N_\infty}{N_0}\right)[1 - \exp(-bt)]\right) \tag{2}$$

where N_∞ is the plateau cell number which is reached at large values of t and the parameter b is related to the initial tumor growth rate. It is convenient to define an auxiliary parameter,

$$k = \ln\left(\frac{N_\infty}{N_0}\right) \tag{3}$$

It follows from Equations 2 and 3 that the time to grow from N_0 to a chosen number of cells, N^* , is given by

$$T^* = -(\ln[-\ln(N^*/N_\infty)/k]) / b \tag{4}$$

We used the Gompertzian function to model the growth kinetics for the primary tumor, the recurrent tumor, and the metastases. However, the general framework of our model is independent of this choice; calculations could be carried out using other functions for $n(t)$.

Even with Gompertzian growth, we suggest that a single set of growth parameters is insufficient to model the clinical data (37). Tumor cells almost certainly have different growth characteristics in different patients, and individual micrometastases within a single patient may also have different growth parameters. Several investigators (37–40) have modeled the variation of tumor growth in the patient population by using a distribution of growth parameters. For our numerical modeling, we followed the example of Norton (37) and used a log-normal distribution of the growth parameter with mean value b and SD σ . N_∞ and N_0 were assumed to be the same for all patients.

For both the deterministic and simulation versions of the model, we assumed that the primary tumor and the local recurrence received a local treatment (*e.g.*, surgery or radiation therapy) within a time which is short compared to the characteristic growth time of any tumor. This process was idealized by assuming that the treatment was “instantaneous.” We further assumed that the growth kinetics of an individual metastasis are unaffected by the treatment.

Deterministic Version. The origin time ($t = 0$) is defined as the time when the primary tumor reaches detectable size, N , and is diagnosed and treated. The growth of the primary tumor begins at an earlier time, $-T_p$, with a single clonogenic cell. T_p is calculated from Equation 4 with $N^* = N$ and appropriately chosen k and b values. If the tumor is locally controlled the treatment (at $t = 0$) reduces the number of clonogenic cells to zero, while for a local relapse the number is reduced to n_0 cells.

As the primary tumor grows, mutations occur, giving some cells metastatic potential (1, 7, 8). A fraction of these cells may escape the tumor, evade the immune system, and form metastatic foci at sites remote from the tumor. To describe the mutation process, we adapted the model proposed by Goldie and Coldman (41) to explain the development of drug resistance. If the number of tumor cells is n and the number of metastatically capable cells is μ then

$$\frac{d\mu}{dn} = \frac{\mu}{n} + \alpha \left(1 - \frac{\mu}{n}\right) \tag{5a}$$

The parameter α (typically $< 10^{-5}$) gives the mutation frequency. The solution

of Equation 5a depends on the initial conditions. For the primary tumor, assuming $\mu = 0$ when $n = 1$ yields

$$\mu(n) = (1 - n^{-\alpha})n \tag{5b}$$

More generally, if $\mu = \mu_0$ when $n = n_0$, the solution is

$$\mu(n) = n \left(1 - n_0^{-\alpha} n^{-\alpha} \left[1 - \left(\frac{\mu_0}{n_0}\right)\right]\right) \tag{5c}$$

Here, μ depends on time and the growth parameters of the primary tumor through its dependence on n . Some of the cells with metastatic potential will escape from the tumor and form micrometastatic foci elsewhere in the patient. In our model, the complicated multistep processes leading to formation of a metastatic focus are lumped into a single “efficiency parameter,” η . The average number of metastatic foci from the primary tumor at time t is given by

$$\frac{dm}{dt} = \frac{\eta d\mu}{dt} \text{ for } t < 0; \quad \frac{dm}{dt} = 0 \text{ for } t > 0 \tag{6a}$$

$$m(t) = 0 \text{ for } t < -T_p \tag{6b}$$

$$m(t) = \eta\mu(t) \text{ for } -T_p < t < 0$$

$$m(t) = m(0) \text{ for } t > 0$$

We need to evaluate the probability that a patient is free of metastatic foci at time t . In the deterministic version of the model, we estimated the probability that the number of metastatic foci is zero with the Poisson distribution, $\exp(-m(t))$.

Each metastasis grows with Gompertzian kinetics, with parameters which may differ from those of the primary tumor. The detectable size for a metastasis, N_m , is reached at a time T_m after the formation of the metastatic focus. T_m is calculated from Equation 4. The probability that a patient is clinically free of distant metastases originating from the primary tumor at any time t is denoted by DMFSP(t). DMFSP(t) is equal to the probability that there are no metastatic foci at the earlier time $t - T_m$. Thus,

$$\text{DMFSP}(t) = \exp(-m(t - T_m)) \tag{7a}$$

DMFSP(t) depends on the growth parameters of both the primary tumor and the metastases. The model can accommodate a distribution of growth constants for the primary tumor and the metastases by averaging Equation 7a over these distributions.

The development of distant metastases originating from a local recurrence is modeled in the same way. The local recurrence grows from n_0 cells which survive the treatment at $t = 0$ until it reaches detectable size in a time T_{LR} . Some fraction of the surviving cells, μ_0/n_0 , may be mutants which already have metastatic potential. Equation 5a is solved with this new initial condition and a parameter α' , which may differ from α , to find the number of metastatically capable cells in the recurrent tumor. The probability of developing a metastatic focus is given by Equation 6a (with, possibly, a different efficiency parameter, η'), holding for $0 < t < T_{LR}$. At any time $t > 0$, the average number of metastatic foci which originated with the local recurrence is m' . The probability that a patient has no metastatic foci from the local recurrence at time $t > 0$ is approximated by $\exp(-m'(t))$. These metastatic foci grow to reach detectable size in a time T_m' , so distant metastasis-free survival relative to the local recurrence is given by

$$\text{DMFSLR}(t) = \exp(-m'(t - T_m')) \tag{7b}$$

As with Equation 7a, Equation 7b may be averaged over a distribution of growth constants for the local recurrence and the metastases.

It is assumed that metastasis-free survival relative to the primary tumor and that relative to the locally recurrent tumors are independent processes. Thus, the overall distant metastasis-free survival is given by

$$\text{DMFS}(t) = \text{DMFSP}(t) \cdot \text{DMFSLR}(t) \tag{7c}$$

To obtain numerical results, it is necessary to select a distribution function for each set of growth parameters being averaged over and to select values for the

appropriate parameters specified in Table 1. In principle, it is possible that the value of the same biological parameter is different for the primary tumor, the recurrence, and the metastases from each. However, the values of some parameters may be quite similar. *e.g.*, N_{∞} , N_{∞}' , $N_{\infty,m}$, and $N_{\infty,m}'$ should be similar. In addition, not all the parameters are needed for fitting some subsets of the clinical data. For example, in fitting the distant metastasis-free survival of locally controlled patients, only 10 parameters are needed and some of them can be assumed to be similar. Thus, the number of independent parameters is not as large as Table 1 suggests. The choices of the growth parameters and other parameters will be further discussed in "Choice of Parameters" and also in connection with the calculation results.

Simulation Version. In this approach, it is convenient to choose $t = 0$ when the primary tumor begins to grow from a single cell. Values for b are selected from a distribution function of growth parameters for the primary tumor, the local recurrence, and the metastases. The distributions may be different for each type of lesion. In this work, we used log-normal distributions with different means and SD.

The growth of the primary tumor in a patient is modeled by choosing a growth parameter according to the assumed log-normal distribution and using Equation 4 to calculate T_p , the time for the primary tumor to grow from a single cell to a detectable size. This time interval is broken into l subintervals of length $\Delta t = T_p/l$ (we used $l = 1000$). At the end of each subinterval, the number of metastatically capable cells in the tumor, μ , is calculated using Equation 5b. The probability of forming a metastatic focus is calculated from

$$P = \eta\mu\Delta t \tag{8}$$

Although the symbol η is used to describe the efficiency of metastasis formation in both the deterministic and simulation versions of the model, the parameter is numerically and dimensionally different in the two versions (dimensionless in Equation 6 and with units of time^{-1} in Equation 8). A random number is selected from a uniform distribution from 0 to 1. If the number generated is less than P , a metastatic focus is formed; otherwise, the simulation proceeds to the next time step. If a focus is established at time $i\Delta t$, a value is chosen from the distribution of growth constants for metastases and Equation 4 is used to calculate the time required for this metastatic focus to reach detectable size, T_m . The difference

$$T^* = (i\Delta t + T_m - T_p) \tag{9a}$$

is the time for detection of the metastasis relative to the time at which the primary tumor is diagnosed. Each time a new metastatic focus is formed, the lowest value of T^* is retained. The process described above is repeated until the primary tumor grows to detectable size. This simulates one patient. For each such patient, the lowest value of T^* is saved, as is the number of metastatic foci for the patient. The lowest value of T^* may be less than zero, corresponding to a patient who presents with distant metastases before the primary tumor is discovered.

The simulation described above is performed for several hundred patients to model metastasis-free survival in patients who are locally controlled. With this approach, we can calculate the percentage of metastasis-free survival as a function of time for these patients. Concomitantly, we can generate "data" on the frequency distribution of the number of metastatic foci.

To simulate a patient with local failure, we assume a value for n_0 , the number of clonogenic cells remaining after treatment of the primary tumor, and for μ_0/n_0 , the fraction of these cells with metastatic potential. If the radiosensitivity of a cell is independent of its metastatic potential, μ_0/n_0 can be found directly from Equation 5b, with $n = N$. The growth constant for the local recurrence is chosen from the distribution of growth constants for the local

recurrence and Equation 4 is used to calculate the time for the local recurrence to reach detectable size, T_{LR} . This growth time is broken into l subintervals of length $\Delta t' = T_{LR}/l$ and the steps described above are repeated, using Equation 5c. The parameters α' and η' for the local recurrence may be different from α and η for the primary tumor, as would be the case if the recurrence is more aggressive than the primary tumor. A metastasis from the local recurrence which grows from a focus formed after i subintervals and which takes a time T_m' to reach detectable size is detected at time $T^{*'} after diagnosis of the primary tumor, where$

$$T^{*'} = (i\Delta t' + T_m') \tag{9b}$$

If the lowest value of $T^{*'}$ is less than the lowest value of T^* for a patient, then $T^{*'}$ determines the duration of metastasis-free survival. In general, the metastasis in question may originate from either the primary tumor ($T^* < T^{*'}$) or the local recurrence ($T^{*' < T^*$).

By repeating the simulation described above for several hundred patients, a histogram of percentage of metastasis-free survival *versus* time for patients with local relapse is generated.

Choice of Parameters. Values for the growth kinetic parameters listed in Table 1 were estimated from published clinical data for prostate cancer (12), using a program developed by Norton (37). This program models clinical data on tumor growth with Gompertzian kinetics, assuming a log-normal distribution of growth parameters. These parameter values were used as guides in the calculations; changes of up to 20% were explored in seeking to match the data on the time dependence of distant metastasis-free survival.

If mutation is an improbable event, the mutation parameter α is a small number. For example, for the development of drug resistance (41) α was estimated to be between 10^{-4} and 10^{-6} . For small α , $\alpha \ln(n) \ll 1$ even for large values of n (*e.g.*, if $n = 10^{10}$ and $\alpha = 10^{-5}$, $\alpha \ln(n) = 2.3 \times 10^{-4}$). Therefore, we can use the approximation $n^{-\alpha} = \exp(-\alpha \ln(n)) \cong 1 - \alpha \ln(n)$, and Equation 5b can be rewritten approximately as

$$\mu(n) \cong \alpha n \ln(n) \tag{5b'}$$

Inserting this into Equation 6b, the average number of metastatic foci from the primary tumor is approximately proportional to $\eta\alpha$. Similarly, in Equation 8, the probability of forming such a focus in time interval $(t, t + \Delta t)$ is proportional to $\eta\alpha$. This product indicates the aggressiveness of the tumor in metastases formation even if the approximation leading to Equation 5b' does not hold. If it is assumed that metastasis formation from the primary tumor is independent of whether the tumor is locally controlled or recurs, the same value of $\eta\alpha$ is used for both cases. Then the product of these two parameters must be consistent with the long term distant metastasis-free survival, DMFS_∞, for the locally controlled patients (*e.g.*, 74% for stage B-C/N0 prostate cancer) (12). On the other hand, if the primary tumor in the group with local relapse is modeled as a more aggressive lesion, two values of $\alpha\eta$ must be chosen, with the larger one being used in modeling the patients with local failure.

For tumors that are not locally controlled, the number of clonogenic cells surviving, n_0 , was assumed to be between 1 and 10^4 . The average fraction of metastatically capable cells, μ_0/n_0 , was assumed to be unchanged by the radiation treatment of the primary tumor, *i.e.*,

$$\frac{\mu_0}{n_0} = \frac{\mu(N)}{N} \tag{10}$$

Again, given that α' is small (10^{-4} to 10^{-6}), Equation 5c is proportional to α' and the probability of forming metastatic foci from the local recurrence is proportional to $\eta'\alpha'$. For an "aggressive" local recurrence this product is larger than that for the primary tumor.

Parameters chosen as described above were used in both the deterministic and the simulation models. The results are presented and compared with the published clinical data (12).

RESULTS

The clinical data used for comparison with the model calculations consist of local relapse and metastasis-free survival curves for patients who were without evidence of metastases at the time of initial diagnosis. However, our model predicts that some fraction, f , of the pa-

Table 1 Biological parameters in the mathematical model^a

	Primary	Relapse	Metastases (primary)	Metastases (relapse)
Growth	b, σ	b', σ'	b_m, σ_m	b_m', σ_m'
Maximum cell no.	N_{∞}	N_{∞}'	$N_{\infty,m}$	$N_{\infty,m}'$
Size detected	N	N'	N_m	N_m'
Metastatic transformation	α	α'		
Metastatic spread	η	η'		

^a n_0 , initial number of cells in local relapse; μ_0 , number of metastatically capable cells in local relapse.

tients present with metastases at the time of diagnosis. Since only $(1 - f)$ of the model patients meet the selection criterion for the published clinical data, the calculated DMFS values were normalized by dividing by $(1 - f)$.

Estimates of the parameters needed for the calculations were obtained from clinical data as described previously. These starting values of the parameters were $N_{\infty} = 3.1 \times 10^{12}$ cells, b (mean value of growth parameter) = 0.0283 month⁻¹, σ (SD of the log-normal distribution) = 0.98, $N = 10^9$ to 10^{10} cells, $N_m = 10^9$ to 10^{10} cells, and $DMFS_{\infty} = 74\%$.

N_{∞} was fixed at 3.1×10^{12} for the primary tumor, recurrence, and metastases. The detection thresholds were kept within the range given above for N (usually set at 5×10^9). For the other parameters, the values given above were used as starting points, from which we searched for parameter sets for which the model calculations gave approximate agreement with the clinical data, first for DMFS in locally controlled patients (Figs. 1 and 2), then for local relapse-free survival in the set of patients who eventually have local failure (see Figs. 4 and 5), and finally for DMFS in patients with local relapse (see Figs. 6 and 7). Both the deterministic and simulation versions of the model gave qualitatively similar results.

Figs. 1 and 2 compare the predictions of the deterministic and simulation versions of the model, respectively, with the clinical data for patients with local control. In both graphs the data points are given by triangles. For both model versions, the calculated curves are "curvier" than the data, tending to underestimate the DMFS at 5–10 years (the calculated DMFS is too low) and overestimate it at longer times. The effect is more pronounced when $b = 0.028$ month⁻¹ is used (Fig. 1, curve 1; not plotted in Fig. 2). Agreement was improved by using lower values of the growth parameter, in the range of 0.020 to 0.023 month⁻¹; these were used for the other curves in these figures. Not much effect was seen from changing the detectable size for the metastases (compare Fig. 1, curves 2 and 3) within the range of 5×10^9 to 10^{10} . The average value of the growth parameter b and the "aggressiveness parameters" ($DMFS_{\infty}$ for the deterministic version and $\alpha\eta$ for the simulation version) are the parameters most sensitive to variation.

In the simulation version, the curves are generated, as described previously, by a process using a random number generator. Different sequences of random numbers could be produced by using different seeds; this was observed to produce DMFS values which differed by $\pm 2\%$, relative to those graphed.

The simulation version generates a frequency distribution for the number of metastatic foci, while in the deterministic version a Poisson distribution is assumed. Fig. 3 compares these two distributions when 70% of the patients (Fig. 3A) and 17% of the patients (Fig. 3B) are free of metastatic foci from the primary tumor at diagnosis [*i.e.*,

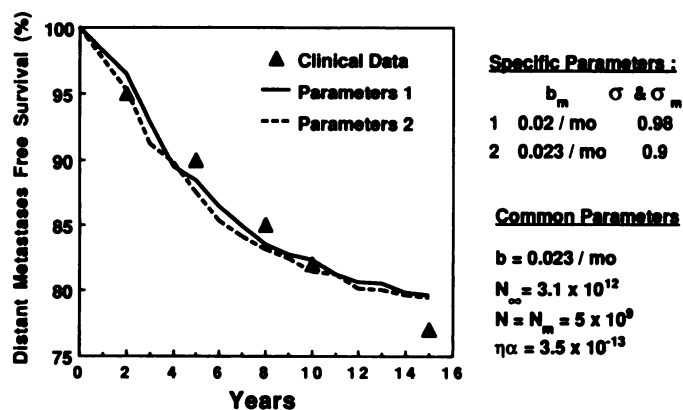


Fig. 2. Comparison of clinical data for DMFS for locally controlled patients with calculations using the simulation version of the model.

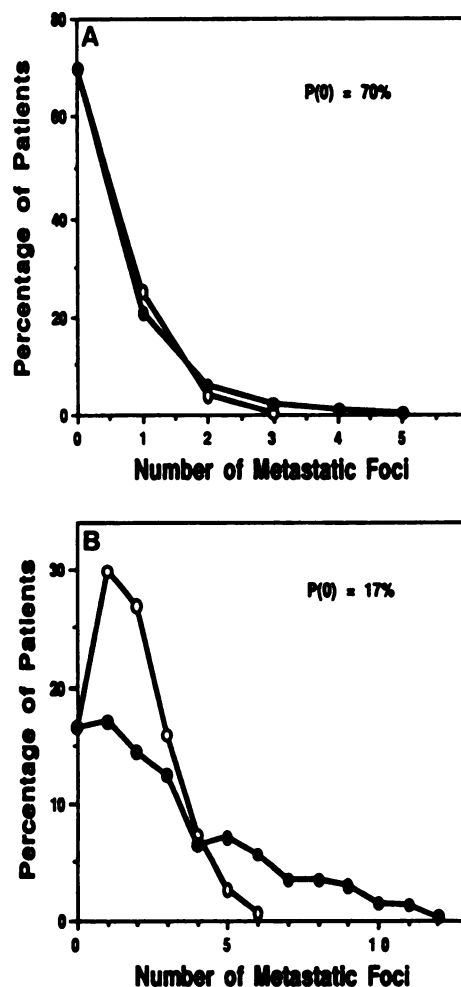


Fig. 3. Comparison of the frequency distribution of the number of metastatic foci generated by the simulation version with the predictions of the Poisson distribution having the same probability of zero metastatic foci, $P(0)$. For $P(0) = 70\%$ there is good agreement (A) but for $P(0) = 16.6\%$ the model frequency distribution has a long "tail" that is not seen for the Poisson distribution (B). A, \circ , simulation prediction; \bullet , Poisson distribution; B, \circ , Poisson distribution, \bullet , simulation prediction.

$P(0) = 70\%$ and 17% , respectively]. With the frequency distribution of Fig. 3A, the long term distant metastasis-free survival ($DMFS_{\infty}$) is 70%, while in Fig. 3B it is 17%. From Fig. 3A it is seen that if $DMFS_{\infty}$ is reasonably large (*e.g.*, 70%) the simulation produces a frequency distribution which is similar to a Poisson distribution. However, as $DMFS_{\infty}$ decreases, the Poisson approximation becomes markedly nar-

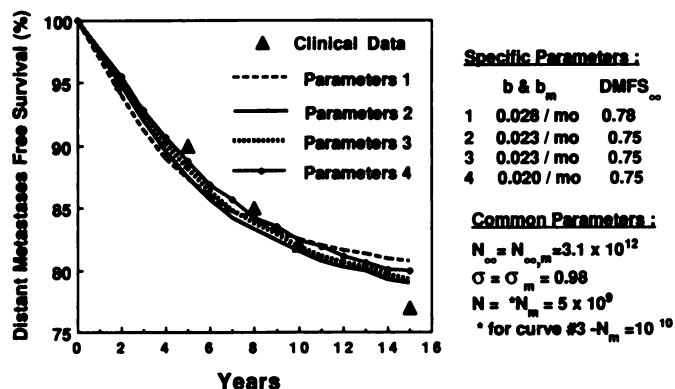


Fig. 1. Comparison of clinical data for DMFS for locally controlled patients with calculations using the deterministic version of the model.

rower than the results of the simulation, as shown in Fig. 3B, and the use of the Poisson distribution to estimate the probability that the number of metastatic foci is zero becomes more questionable.

Figs. 4 and 5 compare the published clinical data for patients with eventual local relapse (12) with calculated values of local relapse-free survival as a function of time, based on the deterministic (Fig. 4) and the simulation (Fig. 5) versions of the model. The clinical data are indicated by triangles. Agreement with the data was approximately the same with $b' = 0.028 \text{ month}^{-1}$ (Figs. 4 and 5, curves 1) and with $b' = 0.023 \text{ month}^{-1}$. Therefore, $b' = 0.023 \text{ month}^{-1}$ was used for the recurrent tumor, to maintain consistency with the growth parameter for the primary tumor. Closest agreement with the data was obtained with a narrower log-normal distribution, using $\sigma' = 0.8$ rather than 0.98 (Figs. 4 and 5, curve 2). Therefore, $\sigma' = 0.8$ was used for the local recurrence in the calculations for metastasis-free survival in patients with local relapse. A larger number of residual tumor cells ($n_0 = 10,000$ versus $n_0 = 1500$) leads to a more rapid decrease in recurrence-free survival, as can be seen by comparing Figs. 4 and 5, curves 3 and 4. A slightly smaller detectable size (Fig. 5, curve 5) improved the agreement in the simulation version.

The predictions of the two versions of the model for DMFS as a function of time for patients with local relapse are shown in Figs. 6 (deterministic) and 7 (simulation). The clinical data of Ref. 12 are indicated by the triangles in these figures. Sixty (18%) of the 328 patients in the plotted data set underwent an orchiectomy or received other hormonal treatment before distant metastases were clinically diagnosed. However, the DMFS in the 268 remaining patients (who received local treatment prior to distant failure) follows a very similar curve, leaving our conclusions unchanged. In Figs. 6 and 7, agreement with the published clinical data is poor if one uses the parameters

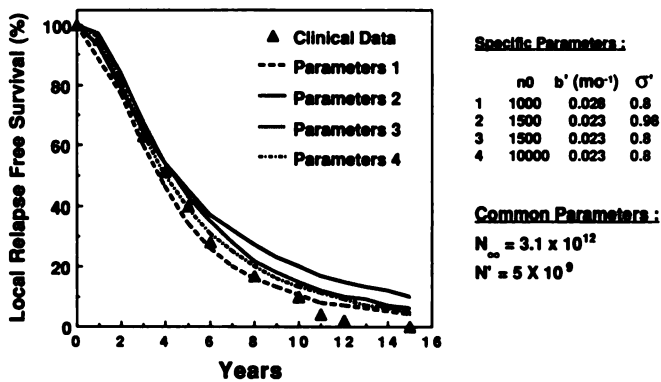


Fig. 4. Comparison of the clinical data for local relapse-free survival with calculations using the deterministic version of the model.

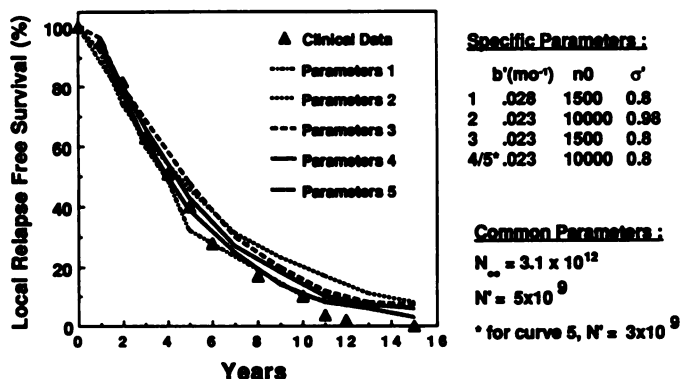


Fig. 5. Comparison of the clinical data for local relapse-free survival with calculations using the simulation version of the model.

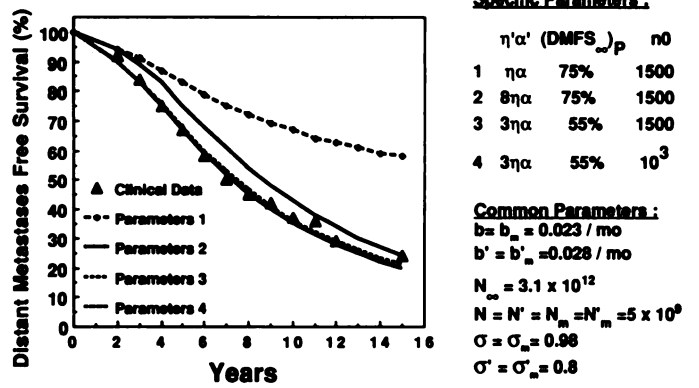


Fig. 6. Comparison of the clinical data for DMFS for patients with local relapse with calculations using the deterministic version of the model.

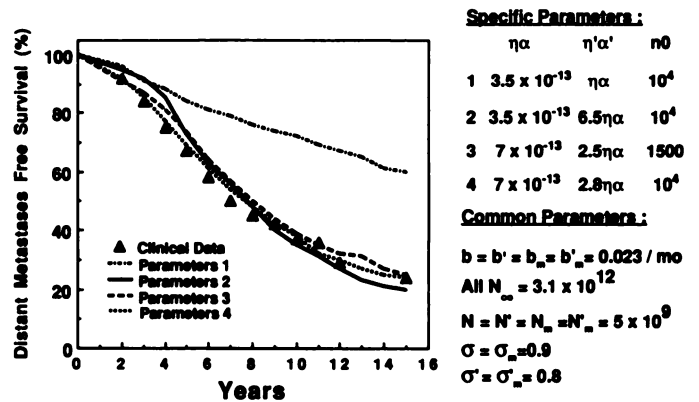


Fig. 7. Comparison of the clinical data for DMFS for patients with local relapse with calculations using the simulation version of the model.

which give a good fit to the DMFS data for locally controlled patients and if one assumes that the local recurrence is equally aggressive in the production of metastases (i.e., $\eta' = \eta$ and $\alpha' = \alpha$). These parameters lead to DMFS curves (parameter set 1) which decline too slowly with time to match the data and also predict too large a value for the long term survival.

There is evidence supporting the hypothesis that the transformation of tumor cells into metastatically capable clonogens requires a sequence of mutations (1, 7, 8). As a result, the residual cells that survive the local treatment may be primed with some of the mutagenic events required for the acquisition of a full metastatic potential and may therefore be more readily transformed to cells which are capable of forming metastatic foci. If this assumption is accepted then the local recurrence may be regarded as more aggressive than the primary tumor in its potential for metastatic dissemination. In our model, this would be represented by $\eta'\alpha' > \eta\alpha$. Combining parameters for the primary tumor which give good agreement with metastasis-free survival data in locally controlled patients with parameters for a more aggressive local relapsing tumor does improve the agreement with the clinical data for incidence of metastases observed in association with local relapse at long time intervals (>10 years) after the initial therapy. However, with these parameters at earlier times, when the effect of metastases originating in the primary tumor dominates, the model curves decrease too slowly to match the data (Figs. 6 and 7, parameter set 2).

The best agreement with the data is obtained by adjusting the aggressiveness of both the primary tumor before therapy and the local relapse, as shown in Figs. 6 and 7, parameter sets 3 and 4. The parameters were changed empirically to improve agreement with the

data at early and late times, and the choice of parameters is not unique. The results are not sensitive to the assumed number of cells which remain after the unsuccessful treatment of the primary tumor, as indicated by parameters sets 3 and 4, which were calculated with $n_0 = 1500$ and $10,000$, respectively.

DISCUSSION

We have developed a theoretical approach that attempts to mathematically model the process of metastasis development. The calculations can be implemented by either a deterministic or a simulation method, with largely similar results. The model assumes Gompertzian tumor growth kinetics with a log-normal distribution of growth constants. Although the model might be expanded to include distributions of other parameters (detectable sizes, $\eta\alpha$, or remaining cells, n_0), we did not consider such factors here.

For calculations, the model requires input values of 10 parameters for the primary tumor and up to 12 additional parameters for recurrent disease. While the number of parameters is large, biological considerations and clinical data constrain the range of variability of many of them. For example, there is a limited range for the number of cells at which tumors and metastases become detectable. Also the number of residual cells with metastatic potential can be estimated based on biological grounds. Two parameters describe the metastatic potential of the primary tumor; α is the rate of developing metastatic potential per mitosis per cell and η is proportional to the rate at which these cells metastasize, entering the bloodstream and forming distant metastatic foci. For the primary tumor in locally controlled patients, the clinical data for long term survival constrain the product of the parameters, $\alpha\eta$. Metastasis formation from locally recurrent disease may be similarly characterized, but the values of these parameters may differ from those chosen for the primary tumor. Our approach was to adjust α , η , α' , and η' in modeling locally recurrent patients to improve agreement with the data.

The above discussion serves to emphasize that our theoretical approach is meant to be a test of the principle that the development of metastases from the primary tumor and the locally recurrent disease can be modeled mathematically using reasonable values of biological parameters. Determination of exact values of the parameters to be used to achieve an optimum fit to clinical data is outside the scope of this investigation.

Within this framework, we were able to find suitable parameters to give a good match to the published clinical data of Fuks *et al.* (12) for distant metastasis-free survival in locally controlled, node-negative stage B and C prostate cancer patients. However, for patients with local relapse, the clinical data were best matched by assuming a somewhat more aggressive primary tumor combined with an even more aggressive local recurrence. Using the set of parameters that produced the best fits to the data (Figs. 6 and 7, parameter set 4), we calculated that approximately 35–45% of the patients developed metastases from the primary tumor and that the recurrent disease further increased the percentage of patients with metastases to about 75%. This means that, if local control could be achieved for all members of this subgroup of patients who initially present without clinical evidence of metastases, their long term metastasis-free survival would be 55–65%, rather than the 24% observed clinically. This is graphically shown by extrapolation of the solid curve in Fig. 8, calculated from the simulation model, to infinite time. Because these patients have a more aggressive primary tumor, they would not do as well as the patients who are presently locally controlled (Fig. 8, circles). However, comparison with the data for distant metastasis-free survival for patients with local relapse (Fig. 8, triangles) shows that achieving local control would more than double the predicted 15-year disease-

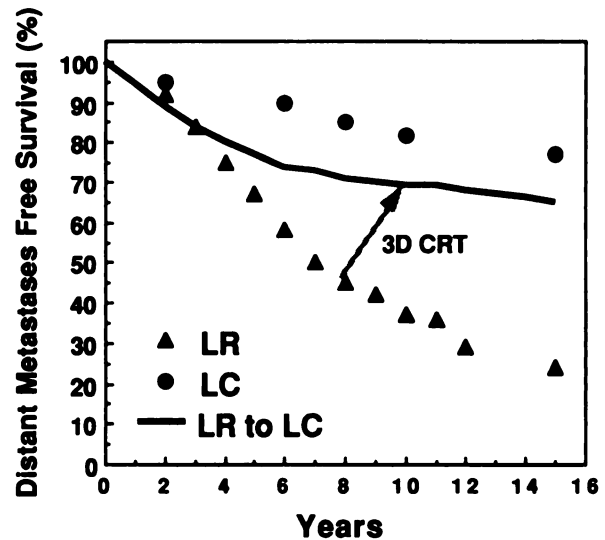


Fig. 8. The simulation version of the model was used to calculate DMFS in a hypothetical situation where local control (LC) is achieved for the cohort of patients who presently relapse locally [for example, by three dimensional conformal radiation therapy (3D CRT)]. The primary tumor parameters of parameter set 4 in Fig. 7 were used to calculate the solid curve. DMFS would be markedly improved, compared to the clinical data for patients with local relapse (LR) (\blacktriangle). However, because parameter set 4 assumes a more aggressive primary tumor than was required to fit the clinical data for locally controlled patients (\bullet), DMFS would still be lower for this group of patients than for the group that is presently locally controlled.

free survival and would also markedly improve the duration of metastasis-free survival at all times after the first few years.

If a parameter set like that discussed above is characteristic of the patients with local relapse, improving the rates of local control with surgery and/or radiation therapy would definitely be advantageous in terms of significantly decreasing the likelihood of metastatic disease. The mathematical model thus indicates that, despite the inherent propensity of prostatic cancer to produce micrometastases prior to initial diagnosis in a fraction of the patients, efforts to improve the efficacy of local treatments and achieve higher rates of local control are justified as a means of preventing the development of metastatic disease in patients who do not have micrometastatic dissemination prior to initial therapy.

REFERENCES

1. Fuks, Z., Leibel, S. A., Kutcher, G. E., Mohan, R., and Ling, C. C. Three dimensional conformal treatment: a new frontier in radiation therapy. In: V. T. DeVita, Jr., S. Hellman, and S. A. Rosenberg (eds.), *Important Advances in Oncology*, pp. 151–172. Philadelphia: Lippincott, 1991.
2. Leibel, S. A., Kutcher, G. J., Mohan, R., Harrison, L. B., Armstrong, J. G., Zelefsky, M. J., LoSasso, T. J., Burman, C. M., Mageras, G. S., Masterson, M. E., Lo, Y.-C., Ling, C. C., and Fuks, Z. Three-dimensional conformal radiation therapy at the Memorial Sloan-Kettering Cancer Center. *Semin. Radiat. Oncol.*, 2: 274–289, 1992.
3. Suit, H., and Urie, M. Proton beams in radiation therapy. *J. Natl. Cancer Inst.*, 84: 155–164, 1992.
4. Myers, M. H., and Ries, L. A. Cancer patient survival rates: SEER program results for 10 years of follow-up. *CA Cancer J. Clin.*, 39: 21–32, 1989.
5. DeVita, V. T. Progress in cancer management. *Cancer (Phila.)*, 51: 2401–2409, 1983.
6. Perez, C. A., and Brady, L. W. Overview. In: C. A. Perez and L. W. Brady (eds.), *Principles and Practice of Radiation Oncology*, Ed. 2, pp. 25–26. Philadelphia: J. B. Lippincott, 1992.
7. Leibel, S. A., Ling, C. C., Kutcher, G. J., Mohan, R., Cordon-Cardo, C., and Fuks, Z. The biological basis of conformal three-dimensional radiation therapy. *Int. J. Radiat. Oncol. Biol. Phys.*, 21: 805–811, 1991.
8. Leibel, S. A., and Fuks, Z. The impact of local tumor control on the outcome in human cancer. In: L. W. Brady, M. D. Donner, H. P. Heilmann, and H. Heuck (eds.), *Medical Radiology: Diagnostic Imaging and Radiation Oncology*. Berlin: Springer-Verlag, in press, 1993.
9. Ramsay, J., Suit, H. D., and Sedlacek, R. Experimental studies on the incidence of metastases after failure of radiation treatment and the effect of salvage surgery. *Int. J. Radiat. Oncol. Biol. Phys.*, 14: 1165–1168, 1988.
10. Sheldon, P. W., Begg, A. C., Fowler, J. F., and Lansley, I. F. The incidence of lung metastases in C3H mice after treatment of implanted tumors with x-rays or surgery. *Br. J. Cancer*, 30: 342–348, 1974.

11. Todoroki, T., and Suit, H. D. Therapeutic advantage in preoperative single dose radiation combined with conservative and radical surgery in different size murine fibrosarcoma. *J. Surg. Oncol.*, 29: 207-215, 1985.
12. Fuks, Z., Leibel, S. A., Wallner, K. E., Begg, C. B., Fair, W. R., Anderson, L. L., Hilaris, B. S., and Whitmore, W. F. The effect of local control on metastatic dissemination in carcinoma of the prostate: long term results in patients treated with I-125 implantation. *Int. J. Radiat. Oncol. Biol. Phys.*, 21: 537-547, 1991.
13. Leibel, A. S., Scott, C. B., Mohiuddin, M., Marcial, V., Coia, L. R., Davis, L. W., and Fuks, Z. The effect of local-regional control on distant metastatic dissemination in carcinoma of the head and neck: results of an analysis from the RTOG head and neck database. *Int. J. Radiat. Oncol. Biol. Phys.*, 21: 549-556, 1991.
14. Chauvet, B., Reynaud-Bougnois, A., Calais, G., Panel, N., Lansac, J., Bougnois, P., and Le Floch, O. Prognostic significance of breast relapse after conservative treatment in node-negative early breast cancer. *Int. J. Radiat. Oncol. Biol. Phys.*, 19: 1125-1130, 1990.
15. Fisher, B., Anderson, S., Fisher, E. R., Redmond, C., Wickerham, D. L., Wolmark, N., Mamounas, E. P., Deutsch, M., and Margolese, R. Significance of ipsilateral breast tumor recurrence after lumpectomy. *Lancet*, 338: 327-331, 1991.
16. Chung, C. K., Stryker, J. A., O'Neill, M., and DeMuth, W. E. Evaluation of adjuvant postoperative radiotherapy for lung cancer. *Int. J. Radiat. Oncol. Biol. Phys.*, 8: 1877-1880, 1982.
17. Malissard, L., Nguyen, T. D., Jung, G. M., Forcard, J. J., Castelain, B., Tuchais, C., Allain, Y. M., Denepoux, R., Lagrange, J. L., Panis, X., Rathelot, P., Chaplain, G., Koehlin, M., and Rozan, R. Localized adenocarcinoma of the lung: a retrospective study of 186 non-metastatic patients from the French Federation of Cancer Institutes-The Radiotherapy Cooperative Group. *Int. J. Radiat. Oncol. Biol. Phys.*, 21: 369-373, 1991.
18. Perez, C. A., Bauer, M., Edelstein, S., Gillespie, B. W., and Birch, R. Impact of tumor control on survival in carcinoma of the lung treated with irradiation. *Int. J. Radiat. Oncol. Biol. Phys.*, 12: 539-547, 1986.
19. Fagundes, H., Perez, C. A., Grigsby, P. W., and Lockett, M. A. Distant metastases after irradiation alone in carcinoma of the uterine cervix. *Int. J. Radiat. Oncol. Biol. Phys.*, 24: 197-204, 1992.
20. Paunier, J. P., Delclos, L., and Fletcher, G. H. Cause, time of death, and sites of failure in squamous cell carcinoma of the uterine cervix on intact uterus. *Radiology*, 88: 552-562, 1967.
21. Perez, C. A., Kuske, R. R., Camel, H. M., Galakatos, A. E., Hederman, M. A., Kao, M. S., and Walz, B. J. Analysis of pelvic tumor control and impact on survival in carcinoma of the uterine cervix treated with radiation therapy alone. *Int. J. Radiat. Oncol. Biol. Phys.*, 14: 613-621, 1988.
22. Kuban, D. A., El-Mahdi, A. M., and Schellhammer, P. F. Prognosis in patients with local recurrence after definitive irradiation for prostatic cancer. *Cancer (Phila.)*, 63: 2421-2425, 1989.
23. Zagars, G. K., Von Eschenbach, A. C., Ayala, A. G., Schultheiss, T. E., and Sherman, N. E. The influence of local control on metastatic dissemination of prostate cancer treated by external beam megavoltage radiation therapy. *Cancer (Phila.)*, 68: 2370-2377, 1991.
24. Merino, O. R., Lindberg, R. D., and Fletcher, G. H. An analysis of distant metastases from squamous cell carcinoma of the upper respiratory and digestive tracts. *Cancer (Phila.)*, 40: 145-151, 1977.
25. Schild, S. E., Martenson, J. A., Jr., Gunderson, L. L., Ilstrup, D. M., Berg, K. K., O'Connell, M. J., and Weiland, L. H. Postoperative adjuvant therapy of rectal cancer: an analysis of disease control, survival and prognostic factors. *Int. J. Radiat. Oncol. Biol. Phys.*, 17: 55-62, 1989.
26. Vigliotti, A., Rich, T. A., Romsdahl, M. M., Withers, H. R., and Oswald, M. J. Postoperative adjuvant radiotherapy for adenocarcinoma of the rectum and rectosigmoid. *Int. J. Radiat. Oncol. Biol. Phys.*, 13: 999-1006, 1987.
27. Perez, C. A., Camel, H. M., Galakatos, A. E., Grigsby, P. W., Kuske, R., Buchsbaum, G., and Hederman, M. A. Definitive irradiation in carcinoma of the vagina: long-term evaluation of results. *Int. J. Radiat. Oncol. Biol. Phys.*, 15: 1283-1290, 1988.
28. Stokes, S., Bedwinek, J., Kao, M. S., Camel, H. M., and Perez, C. A. Treatment of stage I adenocarcinoma of the endometrium by hysterectomy and adjuvant irradiation: a retrospective analysis of 304 patients. *Int. J. Radiat. Oncol. Biol. Phys.*, 12: 339-344, 1986.
29. Gustafson, P., Rooser, B., and Rydholm, A. Is local recurrence of minor importance for metastases in soft tissue sarcoma? *Cancer (Phila.)*, 67: 2083-2086, 1991.
30. Markhede, G., Angervall, L., and Stener, B. A multivariate analysis of the prognosis after surgical treatment of soft tissue tumors. *Cancer (Phila.)*, 49: 1721-1733, 1982.
31. Suit, H. D., Mankin, H. J., Wood, W. C., Gebhardt, M. C., Harmon, D. C., Rosenberg, A., Tepper, J. E., and Rosenthal, D. Treatment of the patient with stage N0 soft tissue sarcoma. *J. Clin. Oncol.*, 6: 854-862, 1982.
32. Skipper, H., Schabel, F., Jr., and Lloyd, H. Dose-response and tumor repopulation rate in chemotherapeutic trials. *Adv. Cancer Chemother.*, 1: 205-253, 1979.
33. Laird, A. K. Dynamics of growth in tumors and in normal organisms. *Natl. Cancer Inst. Monogr.*, 30: 15-28, 1969.
34. Winsor, C. P. The Gompertz curve as a growth curve. *Proc. Natl. Acad. Sci. USA*, 18: 1-7, 1932.
35. Simpson-Herren, L., and Lloyd, H. A. Kinetic parameters and growth curve for experimental tumor systems. *Cancer Chemother. Rep.*, 54: 143-174, 1970.
36. Norton, L., Simon, R., Brereton, H. D., and Bodgen, A. E. Predicting the course of Gompertzian growth. *Nature (Lond.)*, 264: 542-545, 1976.
37. Norton, L. A Gompertzian model of human breast cancer growth. *Cancer Res.*, 48: 7067-7071, 1988.
38. Speer, J. F., Petrovsky, V. E., Retsky, M. W., and Wardwell, R. H. A stochastic numerical model of breast cancer that simulates clinical data. *Cancer Res.*, 44: 4124-4130, 1984.
39. Salmon, S. Kinetic rationale for adjuvant chemotherapy of cancer. In: S. Salmon and S. Jones (eds.), *Adjuvant Chemotherapy of Cancer*, pp. 15-27. Amsterdam: Elsevier/North Holland Biomedical Press, 1977.
40. Heuser, L., Spratt, J., and Polk, H. Growth rates of primary breast cancer. *Cancer (Phila.)*, 43: 1888-1894, 1979.
41. Goldie, J. H., and Coldman, A. J. A mathematical model for relating the drug sensitivity of tumors to their spontaneous mutation rate. *Cancer Treat. Rep.*, 63: 1727-1733, 1979.